





# Polyhydroxybutyrate/Mica Biocomposites: Influence of Filler Content on the Thermal and Mechanical Properties of PHB

Ariadne Gonçalves de Leão<sup>a</sup> , Beatriz Cruz Bastos<sup>b</sup> , Ana Carolina Bastos Rodrigues<sup>a</sup> ,  
Elisângela Pereira Cordeiro<sup>b</sup> , Sílvia Cristina Alves França<sup>c</sup> , Bluma Guenther Soares<sup>c</sup> ,  
Shirleny Fontes Santos<sup>a</sup> , Daniele Cruz Bastos<sup>a\*</sup> 

<sup>a</sup>Universidade do Estado do Rio de Janeiro, 23070-200, Rio de Janeiro, RJ, Brasil.

<sup>b</sup>Universidade Federal do Rio de Janeiro, 21941-909, Rio de Janeiro, RJ, Brasil.

<sup>c</sup>Centro de Tecnologia Mineral, 21941-908, Rio de Janeiro, RJ, Brasil.

Received: November 18, 2024; Revised: February 17, 2025; Accepted: March 29, 2025

Polyhydroxybutyrate (PHB) is a crystalline and linear biopolymer that is biodegradable and biocompatible. However, due to its high crystallinity, PHB is rigid and brittle, limiting its applications. The brittleness of PHB can be reduced by incorporating reinforcing fillers. In this context, this study aimed to produce biodegradable composites based on a PHB matrix and mica, as a filler. Scanning electron microscopy (SEM) revealed the lamellar structure of mica within the PHB matrix. Fourier-transform infrared spectroscopy (FTIR) confirmed characteristic mica vibrations, while X-ray diffraction (XRD) identified crystalline phases from both PHB and the filler. Differential scanning calorimetry (DSC) demonstrated mica's effect on crystallinity. Thermogravimetric analysis (TGA/DTG) showed increased thermal stability, with *Tonset* rising from 144 °C (pure PHB) to 212 °C (PHB/mica 12%) and *Tmax* from 207 °C to 260 °C. Tensile testing indicated reduced stiffness, from 413 MPa (pure PHB) to 333 MPa (PHB/mica 12%). These findings highlight mica's role in modifying PHB's structural, thermal, and mechanical properties, addressing gaps in the literature regarding this composite system.

**Keywords:** *Polymer biocomposites, thermal analysis, muscovita.*

## 1. Introduction

The extensive use of plastic materials has significantly enhanced human life, but the resulting surge in plastic consumption due to population growth has led to severe environmental and resource concerns. Between 1950 and 2015, global plastic waste reached 6.3 billion tons, with only 9% being recycled. Projections indicate that by 2050, the recycling rate will still not exceed 30% of total plastic waste<sup>1-3</sup>.

The continuous production of petrochemical polymers depletes fossil resources, while traditional disposal methods, such as incineration and landfilling, exacerbate pollution and resource depletion. To counter these issues, it is essential to develop biopolymers like polyhydroxyalkanoates (PHAs) and polylactic acid, promoting a shift from a linear to a circular economy and enhancing sustainability. PHAs, particularly polyhydroxybutyrate (PHB), synthesized by microorganisms, exhibit properties making them potential alternatives to petroleum-based plastics. PHB is noted for its high crystallinity, low oxygen permeability, biocompatibility, and biodegradability, making it suitable for biomedical applications. However, PHB's brittleness and low thermal stability are significant limitations, addressable by blending with plasticizers, polymer blending, and reinforced composites<sup>3-8</sup>.

Among the materials that can enhance the performance of PHB, mica, a lamellar-structured aluminosilicate mineral, stands out for its unique properties, such as thermal and mechanical resistance, as well as low gas and moisture permeability. However, despite its promising characteristics, the use of mica in PHB-based composites remains underexplored.

The term "mica" refers to a group of complex aluminosilicate minerals characterized by a lamellar structure and diverse chemical compositions and physical properties. Within this group, three primary subtypes are distinguished: muscovite, phlogopite, and biotite. In northeastern Brazil, significant muscovite reserves exist, but the extraction process is predominantly artisanal, leading to low added value and environmental pollution. Muscovite, with the chemical formula  $\text{KAl}_2[\text{Si}_3\text{AlO}_{10}](\text{OH}, \text{F}_2)$ , has numerous industrial applications, including use in capacitors, insulators, plastic fillers, and pearlescent pigments<sup>9-11</sup>. Mica is commonly employed as a reinforcing additive in polymers to enhance their strength, stiffness, and resistance to heat, chemicals, and radiation. It is primarily utilized in applications requiring temperature insulation and heat shields. Additionally, mica is an effective ingredient for reducing the permeability of hydrocarbons and moisture in industrial coatings and for increasing the strength of nylons, polyesters, and epoxies in polar polymer formulations<sup>12-14</sup>.

\*e-mail: [daniele.bastos@uerj.br](mailto:daniele.bastos@uerj.br)

In the study of Wei et al.<sup>15</sup> a series of polylactic acid (PLA) nanocomposite films were developed by incorporating polydopamine-modified mica (PDA@MICA) as a self-assembling nanofiller to enhance mechanical and thermal properties. The findings revealed that PLA/PDA@MICA nanocomposites exhibit superior mechanical performance. Additionally, thermal performance testing showed that the inclusion of PDA@MICA resulted in an increased crystallinity of 24.78%.

Almeida et al.<sup>11</sup> developed composites based on recycled high-density polyethylene (rHDPE) and muscovite mica, with different rHDE/mica ratios (100/0, 95/5, 90/10, 85/15 and 80/20, weight percentage). The hardness analysis confirmed the action of mica as a reinforcing load in the matrix, but this effect stabilized at around 15%. The TG analysis showed that the 85/15 composite presented slightly better performance than the 80/20, indicating that mica, up to 15%, caused disorganization of the polymer structure instead of reinforcing it.

In another study conducted by Kanabenja et al.<sup>16</sup>, a bio-composite filament for 3D printing was developed by blending Polyhydroxybutyrate (PHB) and Polylactic Acid (PLA) with hydroxyapatite (HA) as a reinforcing agent and polypropylene glycol (PPG) as a plasticizer. Various blends were prepared using melt-extrusion, and their thermal properties and flowability were assessed to optimize 3D printing conditions. The addition of PPG improved processability, and the blend with 10 parts per hundred resin (phr) HA and 10 phr PPG showed excellent printability. However, increasing HA content decreased flowability.

A review of studies on PHB/mineral composites highlights the frequent use of montmorillonite and Cloisite minerals<sup>17-20</sup>. These minerals effectively enhance the thermal and/or mechanical resistance of PHB and other PLA-based composites. Kervran et al.<sup>20</sup> noted that untreated montmorillonite improved PHB's thermal stability more than its treated counterpart, likely due to reduced oxygen permeability from the clay. However, these minerals typically require ultrafine (<45 µm) or nanometric particle sizes<sup>18</sup> and are often chemically treated<sup>17,19</sup> or synthetically produced<sup>21</sup>. In contrast, mica, particularly muscovite, has shown promise in enhancing polymer properties in its natural form, with larger particle sizes (>100 µm) and without chemical treatments, improving properties in different kinds of polymers<sup>11,22</sup>.

Notably, the literature does not contain references to PHB/mica-based composites. In this context, the aim of this study was to produce and characterize biodegradable composites composed of polyhydroxybutyrate (PHB) and mica. By exploring and characterizing this unique combination of PHB and mica, the study offers a sustainable alternative with potential real-world applications, enhancing our understanding of biodegradable composites and their potential to address industry needs for environmentally friendly solutions.

## 2. Experimental Procedures

### 2.1. Materials

Pure, non-commercial Polyhydroxybutyrate (PHB) was acquired from Biomer®P Bioplastik, Germany. The mica used

in this work was provided by the Mineral Technology Center (CETEM) and was collected in the Borborema-Seridó region (encompassing the states of Rio Grande do Norte and Paraíba).

The muscovite was processed using an industrial knife milling method to obtain a particle size of less than 2 mm. The resulting product was separated from impurities using a gravity concentration table, where impurities are removed based on density differences while the material slides over a vibrating table. Subsequently, the purified product was ground in a laboratory knife mill and sieved dry to obtain material with a particle size classification of less than 125 µm<sup>9</sup>.

### 2.2. Composites' preparation

The polymer and muscovite mica were pre-dried in an oven with forced air circulation at 70 °C for 2 hours before processing. The materials were manually mixed, and the PHB/mica composites were prepared in the ratios of 100/0, 95/5, 90/10, and 88/12. Each formulation was produced by hot compression molding at 180 °C and 5 tons for 300 seconds. The sample thickness was controlled using two steel bars with a thickness of 1.36 mm. After hot pressing, the composite was cold compressed to room temperature for 240 seconds at 6 tons. Figure 1 illustrates the experimental setup of composites' preparation.

### 2.3. Characterization

#### 2.3.1. FTIR analysis

Fourier-transform infrared spectra were acquired using a Nicolet 6700 FTIR spectrometer (Thermo Scientific). The formulations were mounted on an attenuated total reflectance (ATR) accessory equipped with a ZnSe crystal prior to scanning. The spectra were obtained with an accumulation of 254 scans.

#### 2.3.2. X-ray diffraction (XRD)

XRD patterns of formulations were obtained with a Bruker AXS D4 diffractometer (Ettlinger, Germany) with CuK $\alpha$  radiation ( $\lambda = 1.5406$  Å) operating at 35 kV and 40 mA. The spectra were recorded at diffraction angles in the range of 4–80° with a step of 0.02° and a counting time of 1s per step.

#### 2.3.3. Scanning electron microscopy (SEM)

The SEM analysis was performed using a Hitachi TM3030 Plus tabletop microscope operating at 15 kV to observe specimens coated with silver. Cryogenically fractured transverse sections of the samples were also evaluated, and the images were obtained at 100 x magnification.

#### 2.3.4. Tensile test

The tensile test was conducted using an Emic universal testing machine (Model DL 1000), with a 5 kN load cell, in accordance with ASTM D638-2003<sup>23</sup>. All tests were performed at a temperature of 23 °C ( $\pm 2$  °C) and a relative humidity of 50% ( $\pm 10$ %), with a deformation rate of 20 mm/min.

#### 2.3.5. Differential Scanning Calorimetry (DSC)

The DSC analysis of the PHB/Mica composites was performed using a NETZSCH device (model 204F1 Phoenix),

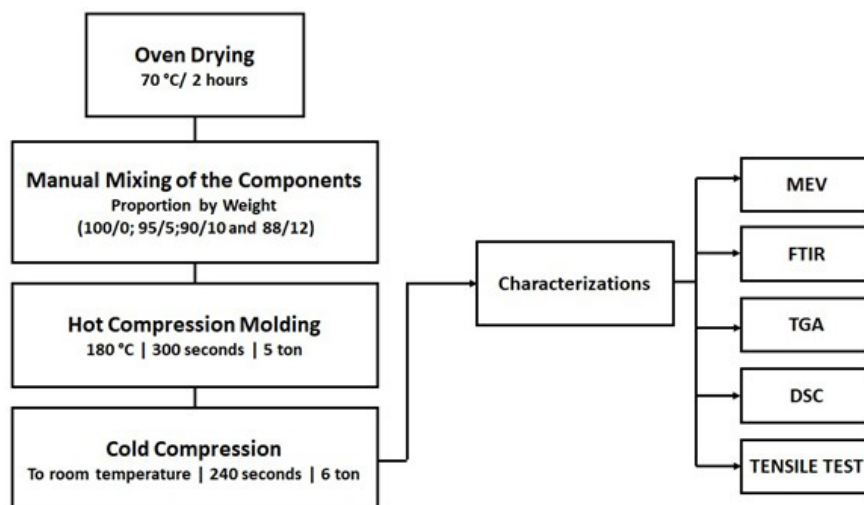


Figure 1. Experimental setup of Composites' preparation.

operating under a nitrogen atmosphere. The differential scanning calorimetry (DSC) analysis was conducted with a Netzsch 204-F1 DSC. The samples (approximately 10 mg each) were heated from 20 °C to 200 °C at a heating rate of 10 °C/min and maintained at this temperature for 2 minutes. Subsequently, a cooling process was carried out at 10 °C/min down to 0 °C. Each sample was then reheated using the same heating rate as in the initial scan.

### 2.3.6. Thermogravimetric Analysis (TGA)

To evaluate the thermal behavior of the PHB/Mica composites, thermogravimetric analysis (TGA) was performed using a TA Instruments device (model Q-50). The heating rate used was 20 °C/min, covering the temperature range from ambient to 600 °C, under an inert nitrogen atmosphere with a flow rate of 60 mL/min.

## 3. Results and Discussion

Figure 2 presents the infrared spectra obtained for the biodegradable composites, neat PHB, and muscovite. In the spectra for PHB and its composites, bands around 2977 and 2935  $\text{cm}^{-1}$  were observed, corresponding to the asymmetric methyl group ( $\text{CH}_3$ ) and the symmetric methylene group ( $\text{CH}_2$ ), respectively. These bands are indicative of the side chains of the PHB monomer<sup>24,25</sup>. A band at 1720  $\text{cm}^{-1}$ , associated with the carbonyl group ( $\text{C}=\text{O}$ ) related to crystalline aggregates, was also noted, with similar results described by<sup>26,27</sup>. The presence of a band at 1380  $\text{cm}^{-1}$  is attributed to the symmetric bending of the methyl group ( $\text{CH}_3$ )<sup>28</sup>. Furthermore, bands between 1300  $\text{cm}^{-1}$  and 1000  $\text{cm}^{-1}$  were observed, which, according to<sup>24</sup>, are related to C-O-C stretching vibrations. Therefore, all these bands observed in the spectra correspond to the chemical bonds of the groups present in the polymer.

According to<sup>11,22</sup>, the vibrations of the mica group can be divided into two regions: a hydroxyl group vibrational region and a network vibrational region, which includes vibrations of  $\text{Si}(\text{Al})\text{O}_4$  tetrahedra, octahedrally coordinated cations, and highly coordinated interlayer cations. This separation is evident for high-energy OH stretching

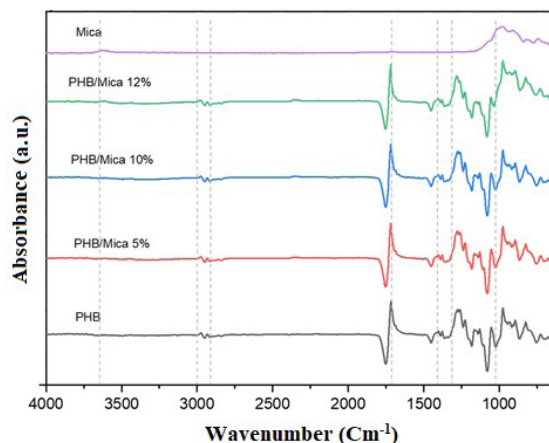


Figure 2. FTIR of PHB, mica and PHB/Mica composite samples.

vibrations, occurring in the 3750-3550  $\text{cm}^{-1}$  region. Absorption bands in the 1200-700  $\text{cm}^{-1}$  region are mainly due to Si-O stretching vibrations. The peaks of the whole composites were unchanged, excepted in composite with 12% of mica, when the presence of a peak in the region of the -OH bonds, characteristic of mica, was observed due to the highest concentration of filler<sup>11,22</sup>.

The bands observed in the FTIR spectra of PHB and its composites confirmed the polymer's chemical structure, as described by<sup>24,25</sup>. The presence of the methyl ( $\text{CH}_3$ ), methylene ( $\text{CH}_2$ ), carbonyl ( $\text{C}=\text{O}$ ), and C-O-C groups aligns with the expected functional groups of PHB. When compared with the literature, such as<sup>13</sup>, the mica vibrations in the hydroxyl and Si-O regions are consistent with the material's characteristics. However, the lack of new or shifted peaks in the composite spectra suggests no chemical interactions between PHB and mica. This observation supports the conclusion that the interface between rHDPE and mica is of a physical nature, as similarly reported in the literature<sup>13,22</sup>. The presence of various functional groups in the mica can potentially influence the interfacial interaction between the filler and the polymer

matrix in the composite and may play a role in determining the mechanical and physical properties of the product.

The diffractograms of pure PHB and the composites are presented in Figure 3. The most intense diffraction peaks related to pure PHB were observed at  $2\theta = 13.4^\circ$  and  $17.1^\circ$ , corresponding to the (020) and (110) lattice planes of the PHB network, respectively<sup>25</sup>. Additionally, a peak at  $19.7^\circ$ , characteristic of the beta crystalline phase according to Wang *et al.*<sup>29</sup>, was observed. Other reflections were also noted in the pure PHB sample at  $21.7^\circ$ ,  $22.4^\circ$ ,  $25.6^\circ$ , and  $26.9^\circ$ , corresponding to the (101), (111), (130), and (040) planes, respectively, consistent with values reported in the literature.

Unlike the FTIR spectra of the composites, the XRD profiles clearly show both the main peaks of muscovite mica at  $8.9^\circ$ ,  $18.1^\circ$ ,  $26.8^\circ$ , and  $45.5^\circ$ , corresponding to the (002), (004), (024), and (029) planes, and the characteristic peaks of PHB, confirming the presence of mica in the materials. Furthermore, these results suggest a good physical interaction between the phases, indicating that the presence of mica did not significantly alter the polymer chain structure or crystallinity. The thermal analysis results support this, showing only a 4% increase in crystallinity for the PHB/Mica 12% composite, a change too small to be detected in the XRD profile<sup>22</sup>. Additionally, a slight increase in the intensity of mica peaks is observed with higher mica concentrations in the composite. This result is expected, as a greater mineral content provides more crystals to undergo refraction, thereby enhancing peak intensity.

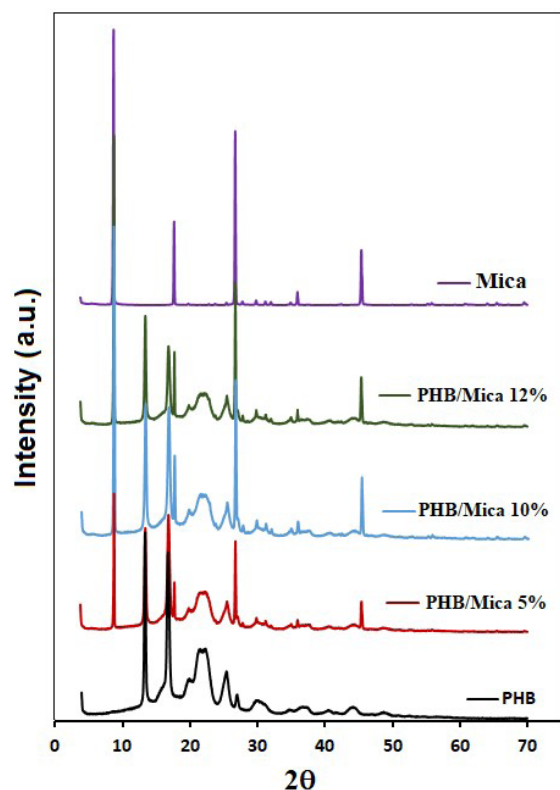


Figure 3. XRD pattern of PHB, Mica and PHB/Mica composite samples.

Figure 4 presents the scanning electron microscopy images obtained for the biodegradable composites of PHB/mica, as well as for the pure polymer. The pure PHB sample (control) exhibits a predominantly homogeneous surface with fractures characteristic of brittle polymers. The absence of additional phases suggests that the material is monophase, highlighting the typical morphology of PHB. It is evident that the morphology of pure PHB was altered with the addition of mica. The composites containing 5%, 10%, and 12% (by mass) of the mineral filler exhibit a random laminar structure characteristic of mica<sup>9,11</sup>, dispersed within the polymer.

With the addition of 5% mica (PHB/Mica 5%), the microstructure begins to show noticeable changes. The presence of mica particles dispersed within the matrix is observed, but the interaction between the reinforcement and the matrix appears to be limited. Small regions of discontinuity indicate weak interfacial adhesion between the mica and the PHB.

When the mica content is increased to 10% (PHB/Mica 10%), the dispersion of particles within the matrix becomes more evident, although some regions show mica agglomeration. The interface between the matrix and the reinforcement appears less homogeneous, suggesting potential points of stress concentration that could negatively affect the material's mechanical properties.

Finally, with 12% mica (PHB/Mica 12%), a higher amount of agglomerated particles is observed, which may indicate reinforcement saturation within the matrix. These agglomerates create regions of structural weakness and further compromise the homogeneity of the material. The interfacial interaction appears to be more severely affected compared to samples with lower mica content, which could have negative impacts on the composite's mechanical performance.

The behavior of the samples with higher mica concentration emphasizes the importance of optimizing the amount of reinforcement, seeking a balance between particle dispersion and interfacial adhesion to improve the mechanical properties and stability of the composite. Similar results were reported by<sup>11</sup>, that used mica as a filler in a high-density polyethylene matrix.

To evaluate the thermal transitions in PHB and its respective composites, DSC analyses were conducted. Figure 5 presents the second heating curves obtained for each sample. The DSC analysis revealed that both the pure polymer and the composites exhibited two endothermic peaks of crystalline fusion ( $T_{m1}$  and  $T_{m2}$ ) at approximately  $152^\circ\text{C}$  and  $165^\circ\text{C}$ , respectively. This behaviour can be attributed to a distribution of crystal sizes within the polymer, indicating crystalline heterogeneity. A similar pattern was observed in the study by<sup>30</sup>, which discussed that the presence of two peaks is likely due to the existence of crystals with lamellae of different thicknesses, with the peak at lower temperature corresponding to the melting of the finer crystals within the polymer.

Figure 5 and Table 1 also show that the melting peaks of composites with 10% and 12% mica exhibit a slight shift toward higher temperatures. This result, combined with the TGA/DTG data, suggests that the addition of mica may enhance the thermal resistance of PHB<sup>30</sup>. Table 1 presents the melting temperatures ( $T_m$ ), melting enthalpies ( $\Delta H_m$ ), and degree of crystallinity ( $X_c$ ) for the pure polymer and



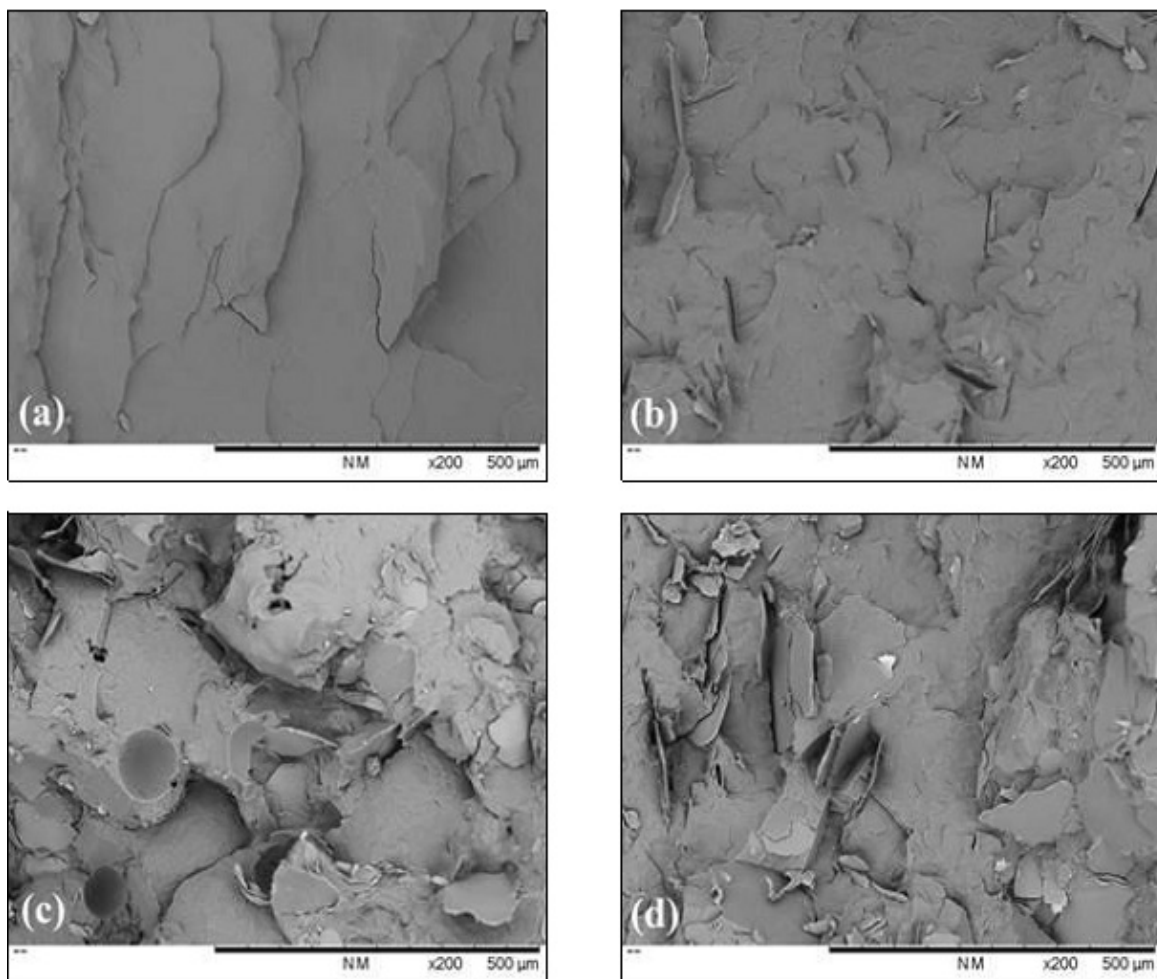


**Figure 4.** SEM images of the analysed composite surfaces: (a) PHB, (b) PHB/Mica 5%, (c) PHB/Mica 10% and (d) PHB/Mica 12%.

composites. The addition of 12% mica led to an approximate 4% increase in crystallinity, indicating that the filler influences the crystallization process of PHB, likely by promoting crystal nucleation.

The DSC results align with the XRD profiles, confirming the melting of crystalline regions observed in both the pure polymer and the composites. However, the slight increase in PHB crystallinity was not detected by XRD, likely because the change (4%) is close to the equipment's detection limit of approximately 2%, which can be higher for hybrid samples and those containing amorphous regions<sup>31</sup>.

Figures 6a and 6b present the TGA and DTG curves obtained for pure PHB and mica-loaded composites and Table 2 provides the initial degradation temperatures ( $T_{\text{initial}}$ ), maximum degradation temperatures ( $T_{\text{max}}$ ), and final degradation temperatures ( $T_{\text{final}}$ ).

The thermograms (Figure 6a) showed that thermal degradation occurred in a single stage for all samples. The presence of muscovite increased the thermal stability of the composites, as evidenced by an increase in  $T_{\text{initial}}$  to 212°C for the composites compared to 144°C for pure PHB.  $T_{\text{max}}$  (Figure 6b) also increased for all composites compared to the polymer, being 261°C and 207°C, respectively. Similar

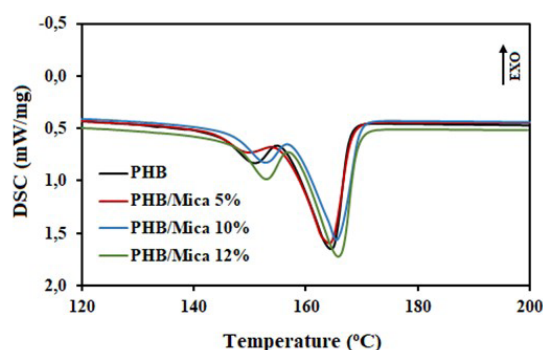


**Figure 5.** DSC of pure PHB and PHB/Mica composites.

behavior was reported by da Silva *et al.*<sup>32</sup> in their study of hybrid composite systems of PHB/zirconia, where the authors discussed that increased thermal stability depends on efficient dispersion of the filler in the matrix.

In this regard, the results indicate a favourable physical interaction between mica and the PHB matrix, contributing to enhanced polymer degradation resistance. Additionally, Santos *et al.*<sup>9</sup> described the thermal stability of mica with

**Table 1.** Percentage composition, melting temperatures ( $T_m$ ), enthalpy of fusion ( $\Delta H_m$ ) and crystallinity ( $X_c$ ) of pure PHB and composites.

Formulation (% m/m)		$T_m$	$\Delta H_m$	$X_c$
PHB	MICA	(°C)	(J.g <sup>-1</sup> )	(%)
100	0	151/164	73	50
	5	150/164	67	48
	10	153/167	68	52
	12	153/167	69	54

**Table 2.**  $T_{onset}$ ,  $T_{max}$  e  $T_{final}$  for the pure PHB e composites samples.

Formulation (% m/m)		$T_{onset}$	$T_{max}$	$T_{final}$
PHB	MICA	(°C)	(°C)	(°C)
100	0	144	207	223
	5	210	261	274
	10	212	261	274
	12	212	260	274

**Table 3.** Results of the tensile test for PHB and its composites.

Sample	Tensile Strength	Elastic Modulus	Strain at break
(% m/m)	(MPa)	(MPa)	(MPa)
PHB	27.00±5.66	413.00±25.45	0.028±0.007
PHB/Mica 5%	25.75±3.40	374.50±11.68	0,027±0.005
PHB/Mica 10%	22.75±0.50	347.00±24.26	0.028±0.001
PHB/Mica 12%	21.25±1.26	333.00±13.64	0.027±0.005

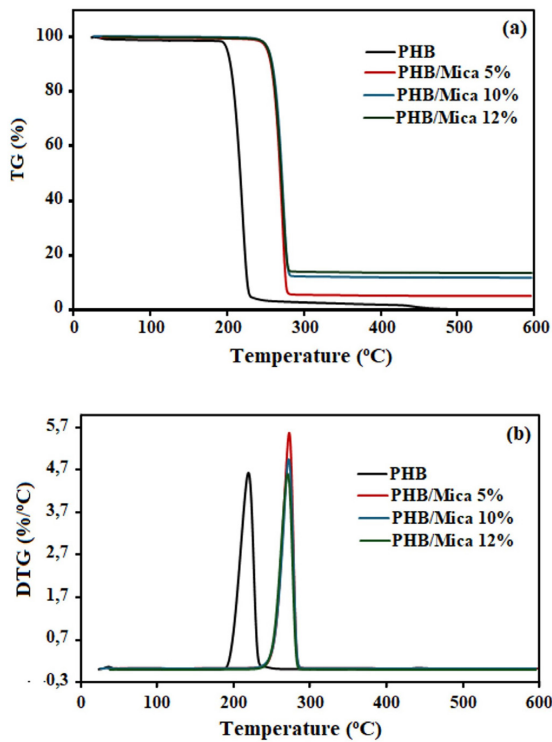


**Figure 6.** (a) TG and (b) DTG of pure PHB and PHB/Mica composites.

an initial temperature of 610°C, which corroborates the TGA results of this study, as the analysis was conducted up to 600°C, a temperature below the onset of degradation for the filler.

The results of the tensile test for PHB and its composites are summarized in Table 3. It can be observed that the elastic modulus decreased with an increase in mica concentration, with the highest filler concentration (12% by mass) showing a 19% decrease in modulus, attributed to the possible non-uniformity in the distribution of the components in the matrix, corroborating SEM results. A slight decrease in the mechanical behavior of the hybrid composites (recycled PP, dimension stone waste, and coconut fiber) in relation to the virgin matrix was observed by Chagas et al.<sup>33</sup>. The response surface methodology revealed that the dimension stone residue content does not significantly influence the mechanical properties results and suggested that the increase in the variable “coconut fiber content” was responsible for improving the mechanical properties of the composite.

In addition, Hyvärinen et al.<sup>34</sup> observed that minor variations in the composition of the recycling of construction and demolition waste filler did not have an impact on the mechanical properties of polymeric matrix, but an increase in the amount of filler increased the deterioration of mechanical properties.

According to Machado et al.<sup>30</sup>, in semicrystalline polymers, there is typically a significant increase in the elastic modulus

as crystallinity degree increases, as observed in the DSC results. However, as crystallinity increases, there may be a broader distribution of crystallite sizes. Smaller crystallites tend to be less effective in resisting deformation, which can result in an overall decrease in the material's elastic modulus.

The DSC results showed that the composite's crystallinity degree increased by 4% with 12% mica compared to neat PHB. However, it is evident that the peak of  $T_m$  (153°C) in this sample is higher than others, supporting the idea that a higher quantity of smaller and irregular crystallites was formed, increasing the heterogeneity of the crystalline phase and thereby reducing the mechanical strength of the composite.

#### 4. Conclusions

In this study biodegradable composites of PHB loaded with 5%, 10%, and 12% m/m of mica were prepared. FTIR analysis revealed characteristic bands of the pure polymer as well as those of the mineral filler, confirming their presence in the composites. X-ray diffraction (XRD) diffractograms showed characteristic peaks of pure PHB, with additional peaks indicating the presence of mica, specifically corresponding to its crystalline planes. Scanning electron microscopy (SEM) evaluated the morphology of the composites, demonstrating a laminar structure dispersed within the polymer matrix, attributed to the presence of mica.

The thermal stability of the composites, compared to pure PHB, was assessed using thermogravimetric analysis (TGA), showing an enhancement due to the mica filler. Thermal analysis by differential scanning calorimetry (DSC) revealed that the filler influenced the crystalline structure of PHB, increasing the crystallinity of the composites and promoting the formation of smaller and irregular crystals. This structural change directly impacted the mechanical properties observed in tensile testing, where the elastic modulus decreased for the composites compared to pure PHB, with a 19% reduction observed for the composite containing the highest concentration of mica (PHB/mica12%).

The enhanced thermal stability, modified crystallinity, and unique morphology of the PHB/mica composites suggest a variety of applications, particularly in sectors seeking biodegradable alternatives as agricultural mulching films, food packaging, medical and pharmaceutical packaging, and others.

This research supports the feasibility of producing PHB/mica biodegradable composites, filling a gap in the literature by providing a detailed analysis of this composite system. Further studies are recommended to explore its full potential across a range of applications.

#### 5. Acknowledgements

The authors acknowledge to CNPq (National Council for Research and Development), and Faperj (Research Support Foundation of Rio de Janeiro).

#### 6. References

- Geyer R, Jambeck JR, Law KL. Production, use, and fate of all plastics ever made. *Sci Adv*. 2017;3(7):e1700782. <http://doi.org/10.1126/sciadv.1700782>.
- Ali SS, Elsamahy T, Abdelkarim EA, Al-Tohamy R, Kornaros M, Ruiz HA, et al. Biowastes for biodegradable bioplastics production and end-of-life scenarios in circular bioeconomy and biorefinery concept. *Bioresour Technol*. 2022;363:127869. <http://doi.org/10.1016/j.biortech.2022.127869>.
- Wang J, Huang J, Liu S. The production, recovery, and valorization of polyhydroxybutyrate (PHB) based on circular bioeconomy. *Biotechnol Adv*. 2024;72:108340. <http://doi.org/10.1016/j.biotechadv.2024.108340>.
- Roa JPB, Patricio PSO, Oréfice RL, Lago RM. Improvement of the Thermal Properties of Poly(3-hydroxybutyrate) (PHB) by Low Molecular Weight Polypropylene Glycol (LMWPPG). *J Appl Polym Sci*. 2012;128(5):3019-25. <http://doi.org/10.1002/app.38484>.
- Phua YJ, Pegoretti A, Araujo TM, Ishak ZAM. Mechanical and thermal properties of poly(butylene succinate)/poly(3-hydroxybutyrate-co-3-hydroxyvalerate) biodegradable blends. *J Appl Polym Sci*. 2015;132(47):42815. <http://doi.org/10.1002/app.42815>.
- Boey JY, Kong U, Lee CK, Lim GK, Oo CW, Tan CK, et al. The effect of spent coffee ground (SCG) loading, matrix ratio and biological treatment of SCG on poly(hydroxybutyrate) (PHB)/poly(lactic acid) (PLA) polymer blend. *Int J Biol Macromol*. 2024;266(Pt 2):131079. <http://doi.org/10.1016/j.ijbiomac.2024.131079>.
- Sahoo BL, Mohanty S, Nayak SK. Synergistic effects of nucleating agent, chain extender and nanocrystalline cellulose on PLA and PHB blend films: evaluation of morphological, mechanical and functional attributes. *Ind Crops Prod*. 2024;215:118614. <http://doi.org/10.1016/j.indcrop.2024.118614>.
- Turco R, Santagata G, Corrado I, Pezzella C, Di Serio M. In vivo and postsynthesis strategies to enhance the properties of PHB-based materials: a review. *Front Bioeng Biotechnol*. 2021;8:619266. <http://doi.org/10.3389/fbioe.2020.619266>.
- Santos SF, França SCA, Ogasawara T. Method for grinding and delaminating muscovite. *Min Sci Technol*. 2011;21(1):7-10. <http://doi.org/10.1016/j.mstc.2010.05.001>.
- Lapčák L, Maňas D, Lapčáková B, Vašina M, Staněk M, Čépe K, et al. Effect of filler particle shape on plastic-elastic mechanical behavior of high-density poly(ethylene)/mica and poly(ethylene)/wollastonite composites. *Compos, Part B Eng*. 2018;141:92-9. <http://doi.org/10.1016/j.compositesb.2017.12.035>.
- Almeida PO, Gerardo CF, de Leão AG, França SCA, Santos SF, Bastos DC. Sustainable composites based on Recycled High-density Polyethylene/mica. *Mater Res*. 2021;24(2):e20200418. <http://doi.org/10.1590/1980-5373-mr-2020-0418>.
- Gan D, Lu S, Song C, Wang Z. Mechanical properties and frictional behavior of a mica- filled poly (aryl ether ketone) composite. *Eur Polym J*. 2001;37(7):1359-65. [http://doi.org/10.1016/S0014-3057\(01\)00010-6](http://doi.org/10.1016/S0014-3057(01)00010-6).
- Gan D, Lu S, Song C, Wang Z. Physical properties of poly(ether ketone ketone)/mica composites: effect of filler content. *Mater Lett*. 2001;48(5):299-302. [http://doi.org/10.1016/S0167-577X\(00\)00318-9](http://doi.org/10.1016/S0167-577X(00)00318-9).
- Panda JN, Bijwe J, Pandey RK. On the significant enhancement in the performance properties of PAEK composite by inclusion of a small amount of nano-mica particles. *Tribol Int*. 2019;136:87-104. <http://doi.org/10.1016/j.triboint.2019.03.033>.
- Wei X, Wei Li W, Li J, Niu X. Mussel-inspired polydopamine modified mica with enhanced mechanical strength and thermal performance of poly(lactic acid) coating. *Int J Biol Macromol*. 2024;273(Pt 2):133148. <http://doi.org/10.1016/j.ijbiomac.2024.133148>.
- Kanabenja W, Passarapark K, Subchokpool T, Nawaukaratharnant N, Román AJ, Osswald TA, et al. 3D printing filaments from plasticized Polyhydroxybutyrate/Poly(lactic acid) blends reinforced with hydroxyapatite. *Addit Manuf*. 2022;59:103130. <http://doi.org/10.1016/j.addma.2022.103130>.

17. Botana A, Mollo M, Eisenberg P, Torres Sanchez RM. Effect of modified montmorillonite on biodegradable PHB nanocomposites. *Appl Clay Sci.* 2010;47(3-4):263-70. <http://doi.org/10.1016/j.clay.2009.11.001>.
18. Iulianelli GCV, Azevedo RS, Silva PSRC, Tavares MIB. PHB nanostructured: production and characterization by NMR Relaxometry. *Polym Test.* 2016;49:57-65. <http://doi.org/10.1016/j.polymertesting.2015.11.011>.
19. Ollier RP, D'Amico DA, Schroeder WF, Cyras VP, Alvarez VA. Effect of clay treatment on the thermal degradation of PHB based nanocomposites. *Appl Clay Sci.* 2018;163:146-52. <http://doi.org/10.1016/j.clay.2018.07.025>.
20. Kervran M, Vagner C, Cochez M, Ponçot M, Saeb MR, Vahabi H. Thermal degradation of polylactic acid (PLA)/polyhydroxybutyrate (PHB) blends: a systematic review. *Polym Degrad Stabil.* 2022;201:109995. <http://doi.org/10.1016/j.polymdegradstab.2022.109995>.
21. Silva RM Jr, Oliveira TA, Araque LM, Alves TS, Carvalho LH, Barbosa R. Thermal behavior of biodegradable bionanocomposites: influence of bentonite and vermiculite clays. *J Mater Res Technol.* 2019;8(3):3234-43. <http://doi.org/10.1016/j.jmrt.2019.05.011>.
22. Bastos BC, Dias ACS, França SCA, Bastos DC, Santos SF. Composites Based on Post-Industrial Wood Plastic Waste and Ultrasonic Treated Muscovite. *Mater Res.* 2023;26(suppl 1):e20220568. <http://doi.org/10.1590/1980-5373-mr-2022-0568>.
23. ASTM: American Society for Testing and Materials. ASTM D638-2003: Standard Test Method for Tensile Properties of Plastics. West Conshohocken: ASTM; 2003.
24. López-Cuellar MR, Alba-Flores J, Rodríguez JN, Pérez-Guevara F. Production of polyhydroxyalkanoates (PHAs) with canola oil as carbon source. *Int J Biol Macromol.* 2011;48(1):74-80. <http://doi.org/10.1016/j.ijbiomac.2010.09.016>.
25. Aguiar LO, Stachewski N, Garcia MCF, Kurek AP, Schneider ALS, Mouga DMDS, et al. Avaliação das propriedades do biopolímero polihidroxibutirato (PHB) extraído por vermes de Zophobas morio Fabricius. *Materia (Rio J).* 2021;26(1):e12938. <http://doi.org/10.1590/s1517-707620210001.1238>.
26. Bhuwal AK, Singh G, Aggarwa NK, Goyal V, Yadav A. Isolation and screening of polyhydroxyalkanoates producing bacteria from pulp, paper, and cardboard industry wastes. *Int J Biomater.* 2013;2013:752821. <http://doi.org/10.1155/2013/752821>.
27. Florez JP, Fazeli M, Simão RA. Preparation and characterization of thermoplastic starch composite reinforced by plasma-treated poly (hydroxybutyrate) PHB. *Int J Biol Macromol.* 2019;123:609-21. <http://doi.org/10.1016/j.ijbiomac.2018.11.070>.
28. Tănase EE, Popa ME, Râpă M, Popa O. PHB/Cellulose fibers based materials: physical, mechanical and barrier properties. *Agric Agric Sci Procedia.* 2015;6(1):608-15. <http://doi.org/10.1016/j.aaspro.2015.08.099>.
29. Wang C, Hsu CH, Wang IH. Scaling laws and internal structure for characterizing electro spun poly[(r)-3-hydroxybutyrate] fibers. *Polymer (Guildf).* 2008;49(19):4188-95. <http://doi.org/10.1016/j.polymer.2008.07.033>.
30. Machado MLC, Pereira NC, de Miranda LF, et al. Estudo das propriedades mecânicas e térmicas do polímero poli-3-hidroxibutirato (PHB) e de compósitos PHB/pó de madeira. *Polímeros.* 2010;20(1):65-71. <http://doi.org/10.1590/S0104-14282010005000011>.
31. Dutrow BL, Clark CM. X-ray Powder Diffraction (XRD) [Internet]. 2007 [cited 2025 Feb 13]. Available from: [https://serc.carleton.edu/research\\_education/geochemsheets/techniques/XRD.html](https://serc.carleton.edu/research_education/geochemsheets/techniques/XRD.html)
32. Da Silva D, de Menezes LR, da Silva PSRC, Tavares MIB. Evaluation of thermal properties of zirconium-PHB composites. *J Therm Anal Calorim.* 2021;143(1):165-72. <http://doi.org/10.1007/s10973-019-09106-7>.
33. Chagas GN, Barros MM, Leão AG, Tapanes NLCO, Ribeiro RCC, Bastos DC. A hybrid green composite for automotive industry. *Polímeros.* 2022;32(2):e2022017. <http://doi.org/10.1590/0104-1428.20220027>.
34. Hyvärinen M, Ronkanen M, Kärki T. The effect of the use of construction and demolition waste on the mechanical and moisture properties of a wood-plastic composite. *Compos Struct.* 2019;210:321-6. <http://doi.org/10.1016/j.compstruct.2018.11.063>.